

AN EFFICIENT ANALYSIS OF LARGE-SCALE PERIODIC MICROSTRIP ANTENNA ARRAYS USING THE CHARACTERISTIC BASIS FUNCTION METHOD

J. X. Wan, J. Lei, and C. H. Liang

School of Electronics Engineering, XiDian University
Xi'an 710071, P. R. China

Abstract—This paper presents a novel approach for the efficient solution of large-scale periodic microstrip antenna arrays using the newly introduced characteristic basis functions (CBFs) in conjunction with the method of moments (MoM) based on the conventional RWG basis functions. The CBFs are special types of high-level basis functions by incorporating the physics of the problem, defined over domains that encompass a relatively large number of conventional subdomain basis functions. The advantages of applying the CBF method (CBFM) are illustrated by several representative examples, and the computation time as well as the memory requirements are compared to those of conventional direct computation. It is demonstrated that the use of CBFs can result in significant savings in computation time and memory requirements, with little or no compromise in the accuracy of the solution.

1 Introduction

2 The Characteristic Basis Function Method

- 2.1 The Mixed Potential Integral Equation (MPIE)
- 2.2 The Characteristic Basis Function Method
- 2.3 Thresholding the Secondary CBFs
- 2.4 The CBFM Solution of Period Microstrip Arrays
- 2.5 The Hybrid Method Combining CBFM with Matched Load Simulation

3 Numerical Results

4 Conclusion

References

1. INTRODUCTION

The method of moments (MoM) has been widely used for the analysis of microstrip structures. However, the conventional MoM using subsectional basis functions and $\lambda/10 \sim \lambda/20$ discretization becomes highly inefficient for the analysis of large or complex antennas and arrays. This is because the size of the associated MoM matrix grows very rapidly as the dimensions become large in terms of the wavelength, or a fine mesh is used to model a complex structure to guarantee good solution accuracy, and this in turn places an inordinately heavy burden on the CPU in terms of both memory and time, which increase with $O(N^2)$, and $O(N^3)$, respectively, in the direct solution, where N is the number of unknowns. When an iterative solver is employed for solving the MoM matrix equation, the operation count is $O(N^2)$ per iteration because of the need to evaluate the matrix-vector multiplication. This operation count is too high for an efficient simulation. To make the iterative method more efficient, it is necessary to speed up the matrix-vector multiplication. There are several techniques developed for this purpose, including the adaptive integral method (AIM) [1], the fast multipole method (FMM) [2–4], the impedance matrix localization (IML) [5], and the conjugate-gradient fast Fourier transform method (CG-FFT) [6]. Recently, the efforts have been made to extend these fast algorithms to microstrip problems. One such example is [7] where the FMM is adopted to analyze scattering from microstrip antennas with the aid of the discrete complex image method (DCIM) [8]. But even the FMM is bounded by a discretization size ranging from $\lambda/10 \sim \lambda/20$, which makes the MoM matrix grow at a rapid pace, as the geometry becomes electrically large.

Another emerging approach for an efficient MoM analysis of microstrip structure is based on the concept of segmentation or domain decomposition, and several techniques have been proposed to implement this concept. For instance, in [9], the modified Diakoptic theory [10], originally proposed for antenna problems, has been secondly applied to microstrip structures, though its use has been relatively limited. The same is true for the diakoptic-theory-based multilevel moments method (MMM) [11], which carries out an iterative basis function refinement to solve passive planar structure problems. The subdomain multilevel approach (SMA), which utilizes the so-called macro basis functions (MBFs) [12], is a novel technique for reducing the matrix size associated with large planar antenna array problems.

In this paper, a novel method for an efficient MoM analysis of large finite period arrays of microstrip antennas using characteristic basis functions (CBFs) is proposed. This technique differs from other

similar approaches, developed previously, in several aspects. First, it includes the mutual coupling effects directly by using a new type of high-level basis function, referred to herein as primary and secondary CBFs, which are used to represent the unknown induced currents on the blocks and solved via the Galerkin method rather than using iterative refinements. Second, it leads to relatively small-size matrices which are sparse as well as well conditioned in nature and are solved directly, unlike other approaches using iterative techniques. Finally, the CBFM is more general, and can be applied to any class of electromagnetic problems. It has been successfully implemented for the analysis of planar microstrip circuits and antennas [13, 14], and radar scattering problems of arbitrary, 3D, faceted surfaces [15]. To show the effectiveness of CBFs, we extend the proposed approach to analyze scattering and radiation from large finite period arrays of microstrip antennas, and the performance factors, for example, the accuracy and numerical efficiency in terms of computation time, are evaluated by comparison with conventional and direct MoM computation. Because in this class of problems, we can take advantage of identical block geometries and spacings between the array elements to generate the CBFs and reduced matrices in a numerically efficient manner. Hence more time can be saved in this work than that in the existing application of CBFM. At the same time, the memory requirements are also reduced dynamically and this seems to be very difficult in [15].

In addition, to extract S parameters of microstrip antennas, a hybrid method combining CBFM with matched load simulation [16] is also introduced in this paper and the time for generating CBFs and filling and solving the reduced matrix will be reduced dynamically because only one port need be fed even if the properties of symmetry and reciprocity are not satisfied. Hence our method is more efficient than one combining CBFM with open load simulation in [13, 14]. Numerical examples are given to illustrate the accuracy and robustness of this method.

2. THE CHARACTERISTIC BASIS FUNCTION METHOD

2.1. The Mixed Potential Integral Equation (MPIE)

The mixed potential integral equation (MPIE) [17], using the formulation of the spatial-domain MoM for a general microstrip structure, can be expressed in matrix form as [18]:

$$ZI = V \tag{1}$$

in which V is an $N \times 1$ known excitation vector, I is the unknown solution vector of size $N \times 1$, and Z is the impedance matrix of $N \times N$ with elements given by

$$Z_{ij} = j\omega \int_{T_i} \int_{T_j} \left[\vec{f}_i(\vec{r}) \cdot \overline{\overline{G}}_A(\vec{r}, \vec{r}') \cdot \vec{f}_i(\vec{r}') - \frac{1}{\omega^2} \nabla \cdot \vec{f}_i(\vec{r}) \nabla \cdot \vec{f}_i(\vec{r}') G_q(\vec{r}, \vec{r}') \right] dr' dr \quad (2)$$

where \vec{f}_i and \vec{f}_j represent the testing and basis function, respectively, T_i and T_j denote their supports, $\overline{\overline{G}}_A$ is the Green's function for vector potential, and G_q is the Green's function for scalar potential.

2.2. The Characteristic Basis Function Method

For electrically large geometries, the size of N becomes prohibitively large when RWG bases are employed, and this rules out the option of direct matrix inversion for extracting the solution of Eq. (1). When an iterative solver is employed for solving Eq. (1), the operation count is $O(N^2)$ per iteration because of the need to evaluate the matrix-vector multiplication. This operation count is too high for an efficient simulation. Techniques such as FMM speed up the matrix vector product, but even the FMM is bounded by a discretization size ranging from $\lambda/10 \sim \lambda/20$, which makes the MoM matrix grow at a rapid pace, as the geometry becomes electrically large.

In view of above, it is of great advantage if the number of unknowns can be reduced or compressed for electrically large structures, as this would considerably reduce the computational time. We employ a novel technique, namely, the characteristic basis function method (CBFM) to address this specific issue. The CBFM is a general approach for dealing with the matrix equations of the form given in Eq. (1), and is independent of the type of basis/testing functions as well as of the field integral equation used to formulate the problem. The first step in the CBFM is to segment the original geometry into smaller blocks, say, M in number, which are fractions in size of the original geometry. Typically, two types of CBFs are defined for each section, namely, the primary and the secondary, though higher-order (for example, tertiary) basis functions may also be included, if necessary. The primary CBFs are solutions for the induced current in the isolated blocks, whereas the secondary CBFs account for the field coupling between the blocks. The CBFs are generated by solving relatively small-size matrix equations, as compared to the original matrix. Hence, the time needed to generate these CBFs is usually reasonably small.

In general, the level of field coupling between the blocks is governed by such parameters as the geometry and the frequency, and we can take advantage of this fact by discarding some of the secondary CBFs, in a dynamic manner, by using a thresholding scheme. Then, the set of primary and secondary CBFs are employed as high-level basis and testing functions to generate a reduced matrix via the use of the Galerkin method. This matrix is typically quite small and thus can be solved directly and yet does not sacrifice the accuracy of the solution in the process. In addition, the use of CBFs does not result in a deterioration of the condition number of the matrix, as is often the case with other entire domain basis functions, which also serve to reduce the matrix size.

1	5	9	13
2	6	10	14
3	7	11	15
4	8	12	16

Figure 1. Geometry of a rectangular patch divided into 16 blocks.

To illustrate the CBF method, a rectangular microstrip antenna which is divided into 16 blocks is shown in Figure 1, with no real limitation placed on the size of the individual domain. Next, we proceed to construct a set of basis functions that are characteristic of that particular domain (patch in this example). These characteristics basis functions (CBFs) are comprised of (i) primary bases arising from the self-interactions from within the domain, and (ii) secondary basis functions that account for the mutual coupling effects from the rest of the domains.

In the first step, the primary CBF of each block is constructed. Let N_i be the number of unknowns in block i . For the purpose of generating the CBFs, we first extend this block by Δ all directions, as shown in Figure 1 for $i = 6$ and $i = 16$. Let N_i^e be the number of unknowns in this extended block. Our next step is to extract the coefficient matrix $Z_e^{(i)}$ for the extended block, whose size is $N_i^e \times N_i^e$, from the MoM matrix Z . This block matrix is subsequently used for generating the CBFs for the block i . The primary basis $J_i^{(i)}$ for this

block are generated by solving the following equation [15]:

$$Z_e^{(i)} J_i^{(i)} = R^{(i)} \quad i = 1, 2, \dots, M \quad (3)$$

where, $R^{(i)}$ is a subset of the original excitation vector V , and is formed by extracting those N_i^e rows belonging to block i , and $M = 16$.

Even though the original number of unknowns N may be quite large because the original patch geometry is large in terms of the wavelength, the number of unknowns in each block can be still be kept to a manageable size and, hence, Eq. (3) can be solved by using LU decomposition without the need to resort to iterative techniques. This type of factorization is highly desirable since we need to solve (3) repeatedly to obtain the secondary basis functions in the next step (see below). To construct the primary bases, we solve Eq. (3) for each of the individual blocks, $i = 1, 2, \dots, M$, to complete the set.

Having constructed the primary bases, we proceed next to generate the secondary ones that account for the mutual coupling between various blocks. For each block, the secondary bases are constructed from Eq. (3), but with different excitations. For a geometry that is divided into M blocks, we generate M primary bases. For each of these blocks, there are $M - 1$ secondary bases, which are obtained by solving the following equation:

$$Z_e^{(i)} J_k^{(i)} = R_k^{(i)} \quad k = 1, 2, \dots, i - 1, i + 1, \dots, M \quad (4)$$

where $J_k^{(i)}$ is the k^{th} secondary basis for block i , and $R_k^{(i)}$ is the excitation vector resulting from the mutual coupling between block i and block k . Even though the original blocks do not overlap with each other, Eq. (4) deals with an extended block, and they do overlap. In view of this, two distinct cases are identified for generating $R_k^{(i)}$.

In the first case, there is no overlap (no common unknowns) between the extended block i and block k . In such a scenario, the excitation vector resulting from the mutual coupling between these two blocks is given by

$$R_k^{(i)} = -Z^{(i,k)} J_k^{(k)} \quad (5)$$

where $Z^{(i,k)}$ is a $N_i^e \times N_k$ matrix formed from MoM matrix Z by selecting the testing location at the extended block i , with the source location being the block k .

In the second case, the extended block i shares some of the unknowns with the block k and we let $N_{i,k}^{(c)}$ be that number. We identify and eliminate these source locations from $Z^{(i,k)}$ and $J_k^{(k)}$, thus making

them $N_i^e \times (N_k - N_{i,k}^{(c)})$ and $(N_k - N_{i,k}^{(c)}) \times 1$ respectively. Note that the size of $R_k^{(i)}$ remains $N_i^e \times 1$, in this case also. Once we find the excitation vector $R_k^{(i)}$ resulting from the mutual coupling, the secondary basis for the block i is computed from Eq. (4), making use of the already factored matrix $Z_e^{(i)}$.

Extensive numerical experiments have shown that the inclusion of second-order coupling (secondary CBFs) is adequate for producing accurate results, though higher-order bases may be added on as-needed basis, if desired. Once the CBFs for each of the blocks have been generated, we ortho-normalize them by using the modified Gram — Schmidt procedure with regards to each other in order to improve the condition number of the reduced matrix. The solution to the entire problem is then expressed as a linear combination of the CBFs as follows:

$$[I] = \sum_{k=1}^{M^2} \beta_k [I_k^c] \quad (6)$$

where $[I_k^c]$ is the k^{th} CBF, and β_k is the coefficient of k^{th} CBF. By inserting (6) into (1) and using the adjoint of $[I^c]$ as the testing function, we obtain

$$[I^c]^+ [Z][I^c][\beta] = [I^c]^+ [V] \quad (7)$$

or, in a simpler form

$$[Z^c][\beta] = [V^c] \quad (8)$$

where $[I^c]$ is the matrix form of CBFs of dimension $N \times M^2$, $[\beta]$ is the coefficient vector of dimension $M^2 \times 1$. Typically M^2 , the dimension of the reduced matrix, is much smaller than that of the original matrix equation (N), and the reduced matrix equation can be solved directly. Once the coefficients of the reduced matrix equation have been obtained, the solution for the original problem is readily recovered from the equation:

$$[I] = [I^c][\beta] \quad (9)$$

Once this solution is constructed, the parameters such as the scattering parameters, the scattered field, radar cross section, etc., can be easily computed.

2.3. Thresholding the Secondary CBFs

The level of field coupling between the blocks is governed by such parameters as the geometry and the frequency, and some of the secondary CBFs can be discarded in a dynamic manner by employing a thresholding scheme. The decision whether or not to include a secondary CBF is based on the following criterion:

$$\begin{cases} \text{Use} & \text{if } \|I_{\text{sec}}\|/\|I_{\text{pri}}\| \geq \varepsilon \\ \text{Discard} & \text{if } \|I_{\text{sec}}\|/\|I_{\text{pri}}\| < \varepsilon \end{cases} \quad (10)$$

where $\|I_{\text{sec}}\|$ is the vector-2 norm of the secondary CBF induced by I_{pri} , $\|I_{\text{pri}}\|$ is the vector-2 norm of the primary CBF, and ε is the threshold value. The set of primary and secondary CBFs obtained by applying the above criterion includes only the dominant secondary CBFs, and this process minimizes the number of total CBFs without sacrificing the accuracy. The dimension of the reduced matrix, constructed by using the set of CBFs as the basis and the testing functions, is relatively small; hence the matrix can be easily solved by direct methods.

2.4. The CBFM Solution of Period Microstrip Arrays

In this paper, we focus on the application of CBFM in large-scale period microstrip arrays. In these structures, we can take advantage of identical block geometries and spacings between the array elements to generate the CBFs and reduced matrices in a numerically efficient manner. For example, we consider a period array divided into M blocks. In fact, only the interaction between the first block and other blocks need computing, and then they can be used repeatedly to express the interactions among other blocks. Hence the memory and computing requirements are only $1/M$ of those of conventional direct computation. In addition, the time for generating CBFs and filling and solving the reduced matrix will be also reduced dynamically in these applications. For example, for the primary CBFs, we can copy the solution of the first block for the other blocks. For the secondary CBFs and reduced matrices, we do the LU factorization only once for the first block and use it later-repeatedly-to avoid redundant computation.

2.5. The Hybrid Method Combining CBFM with Matched Load Simulation

The CBFM has been successfully implemented for the analysis of planar microstrip circuits and antennas [13], For N port circuit problems, it is necessary to extract the scattering parameters. In

general, N linearly independent excitations are required for N port network if microstrip structures are analyzed with open load simulation. In this case, NM CBFs are necessary if the properties of symmetry and reciprocity are not satisfied. However, the analysis combining CBFM with matched load simulation [16] is adopted to extract the scattering parameters in this paper. In this method, only M CBFs are constructed because only one port is excited even if the properties of symmetry and reciprocity are not satisfied. Thus the number of CBFs and the size of the reduced matrix are reduced and the time for generating CBFs and filling and solving the reduced matrix will be also reduced dynamically because the CPU time is proportional to the number of CBFs in the CBFM.

3. NUMERICAL RESULTS

To illustrate the validity and accuracy of the method described above, we present several typical numerical examples. All of the computations are performed on a PC equipped with 512 MB of RAM and a 2.4 GHz processor. As a first example, we consider a 4×1 patch array fed by microstrip lines as shown in Figure 2. Each element consists of a rectangular patch with a length and width of 50 and 45 mm, respectively, and a 50Ω feed line whose width and length are 5 and 75 mm, respectively. The feed inset for the patch has a width of 5 mm and a length of 12.5 mm, and is optimized to match a 50Ω feed line. The array is placed on a substrate whose thickness is 1.6 mm and dielectric constant is 2.2, and a center-to-center separation between the elements of 90 mm. In this example, the array elements are geometrically isolated and each of them is identified as a separate block, hence the number of blocks is four.

A conventional approach to modeling this antenna requires 2516 unknowns if the RWG basis functions are used, because each of the four blocks has 629 unknowns. Since the array elements are isolated, the partitioning of the blocks is intuitively obvious. The array has an expected resonant frequency slightly above 2 GHz, and the proposed CBF method is implemented over the frequency range 1.8–2.7 GHz. In this paper, the hybrid method combining CBFM with matched load simulation [16] is proposed to extract S parameters of microstrip antennas. Because only one port is fed, only 4 CBFs are constructed if all of the secondary CBFs are generated with no thresholding. However using the method in [13], a total number of 16 CBFs will be generated. Thus our method is more efficient and the computational time for the CBFM will be reduced dynamically. The magnitude of the S parameters are shown in Figures 3 and compared with the direct MoM

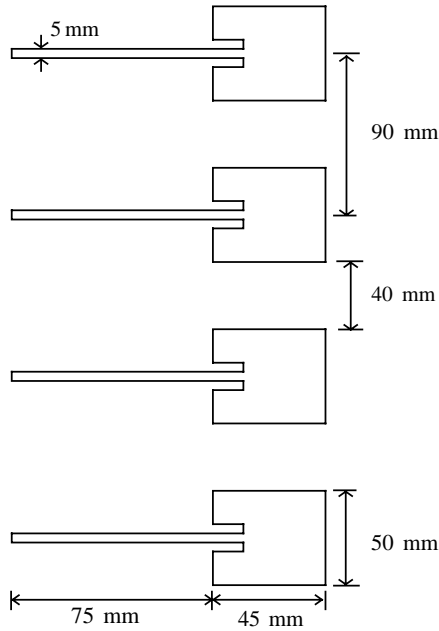


Figure 2. Geometry of a 4×1 patch array fed by microstrip lines.

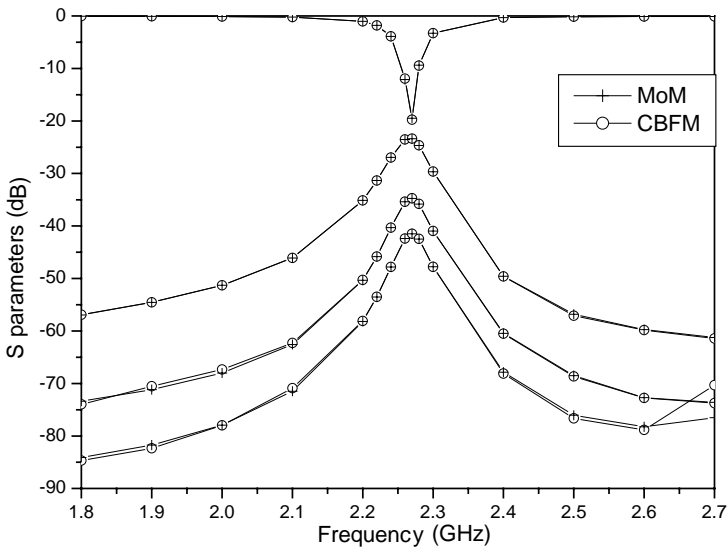
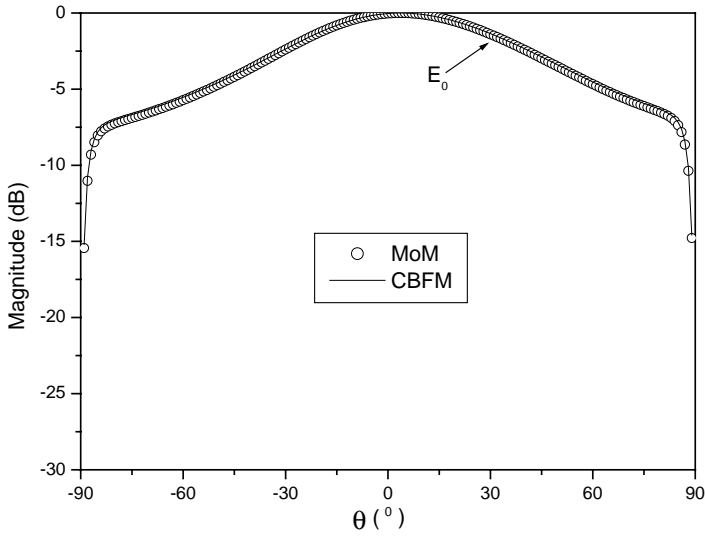


Figure 3. Comparison of the magnitude of the S parameters for the 4×1 patch array fed by microstrip lines.

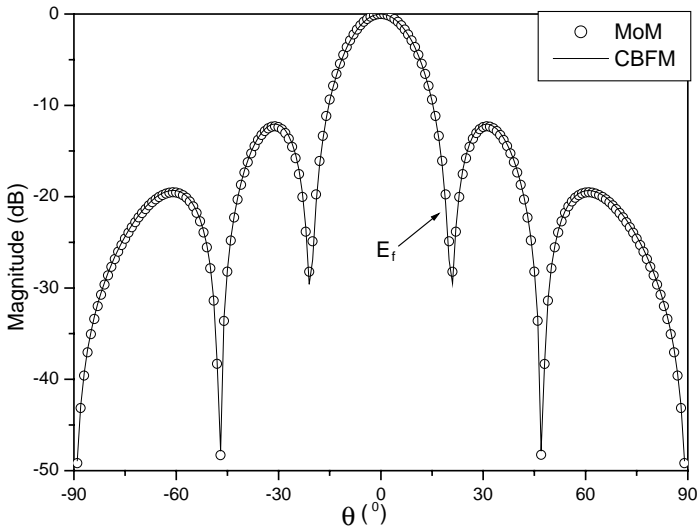
solutions. We observe that, except for minor differences in the S_{41} parameters at off-resonance frequencies where their levels are very small (below -65 dB) — all of the S parameters match very well with those predicted by the direct solution.

To full-wave analysis of radiation from this antenna, four ports must be all fed and lead to 16 CBFs. To generate efficiently the CBFs and reduced matrices, we take advantage of identical block geometry and spacing between the array elements in order to save computation time. For the primary CBFs, we can copy the solution of the first block for the other blocks. For the secondary CBFs and reduced matrices, we do the LU factorization only once for the first block and use it later-repeatedly-to avoid redundant computation. The radiation patterns are shown in Figure 4 at 2.27 GHz. For this example, the direct solution time for each frequency is 1008.15s, whereas it is only 197.07s when the proposed CBF method is used.

Then we consider the plane wave scattering from three finite arrays of microstrip patch antennas. The element of the arrays is a rectangular patch with 36.6 mm width and 26.6 mm length. The distance between two adjacent elements in both the x and y directions is 55.517 mm. The geometry can be obtained from [19] and is shown in Fig. 5(a). The substrate parameters are $h = 1.58$ mm and $\varepsilon_r = 2.17$. The patch is illuminated by an θ -polarized incident plane wave traveling along the direction of $\theta^i = 0^\circ$ and $\varphi^i = 45^\circ$. Three various size arrays (3×3 , 7×7 and 11×11) are analyzed from 2 to 4 GHz in steps of 50 MHz leading to a total of 41 frequency points. For these examples, the array elements are again geometrically isolated and we can have different choices to how to divide these structures into blocks. Two possible schemes are shown in Figure 5(a) and (b). In Figure 5(a), the array is divided into k^2 blocks and leads to k^4 CBFs and a reduced matrix of size $k^4 \times k^4$. However, the array is divided into k blocks and leads to k^2 CBFs and a reduced matrix of size $k^2 \times k^2$ in the second scheme (see Figure 5(b)). It is clear that these two schemes have both own advantages. On the one hand, the memory and computing requirements are only $1/k^2$ of those of conventional direct computation, but a large-size reduced matrix is led to in the first scheme. For example, the size of the reduced matrix is 2401×2401 and 14641×14641 for the 7×7 and 11×11 arrays respectively if all of the secondary CBFs are constructed with no thresholding, hence the direct LU decomposition of these reduced matrices is very expensive or impossible. On the other hand, though the size of reduced matrices is very small in the second scheme, the memory and computing requirements are k times more than those in the first one. Hence according to the discussions above, if the mutual

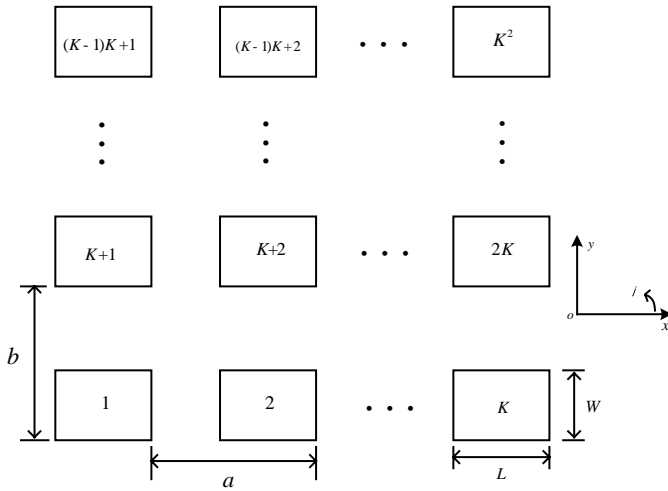


(a)

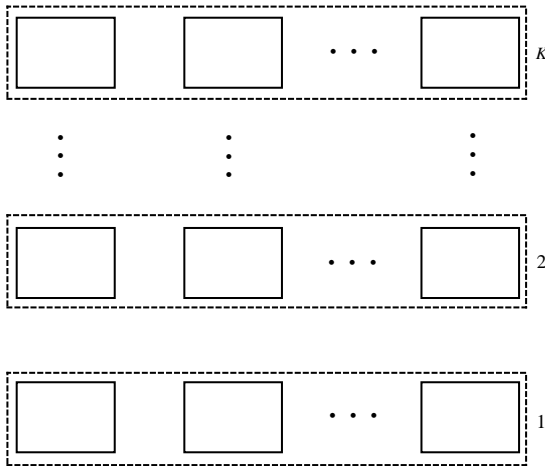


(b)

Figure 4. Comparison of the radiation patterns at 2.27 GHz for the 4×1 patch array fed by microstrip lines: (a) $\varphi = 0^\circ$ cut; (b) $\varphi = 90^\circ$ cut.



(a) The first scheme



(b) The second scheme

Figure 5. Geometry of a finite array of rectangular microstrip patches and two different divided schemes for this array: (a) the first scheme; (b) the second scheme.

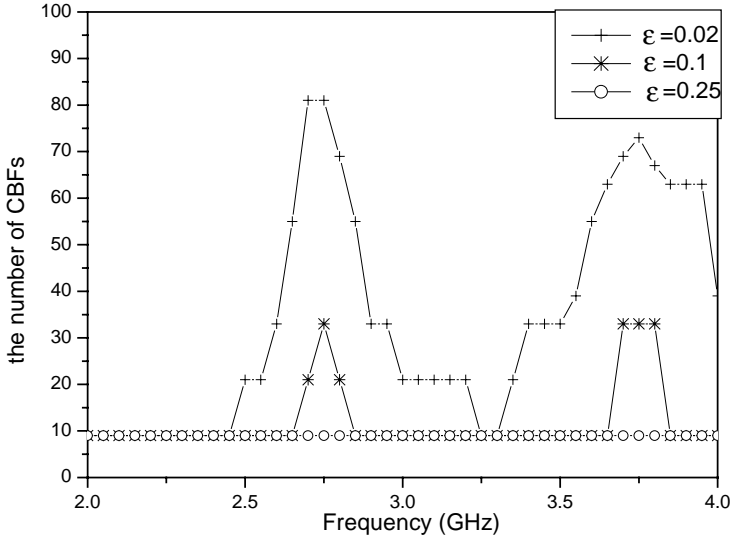


Figure 6. The number of CBFs as functions of the frequency for the 3×3 array.

couplings between the blocks is very weak and a lot of the secondary CBFs can be discarded, then the first scheme is more suitable, or the second one should be chosen. Hence, we should firstly determine how much the mutual couplings between the blocks are. As an example, the 3×3 array is considered and divided into 9 blocks according to the first scheme. We select $\epsilon = 0.25$, $\epsilon = 0.1$ and $\epsilon = 0.02$ respectively, and the number of CBFs as functions of the frequency is shown in Fig. 6. Note that a larger number of secondary CBFs are needed near the resonance frequency due to stronger mutual couplings between the blocks. However, we also found that even if at the resonance frequency, the secondary CBFs considering the strongest mutual couplings are still much less than a quarter of the primary CBFs, thus we can discard all the secondary CBFs and only use the primary CBFs to construct the solutions in this example. To illustrate this, the RCS as a function of frequency is presented in Fig. 7, and the solutions of the only primary CBFs show an excellent agreement with that of CBFM including the mutual coupling effects and the MoM results over the entire frequency band. And a similar conclusion can be drawn for the 7×7 and 11×11 arrays.

Since the only primary CBFs can give the accurate solutions, hence the first scheme is chosen in this paper, and these three arrays

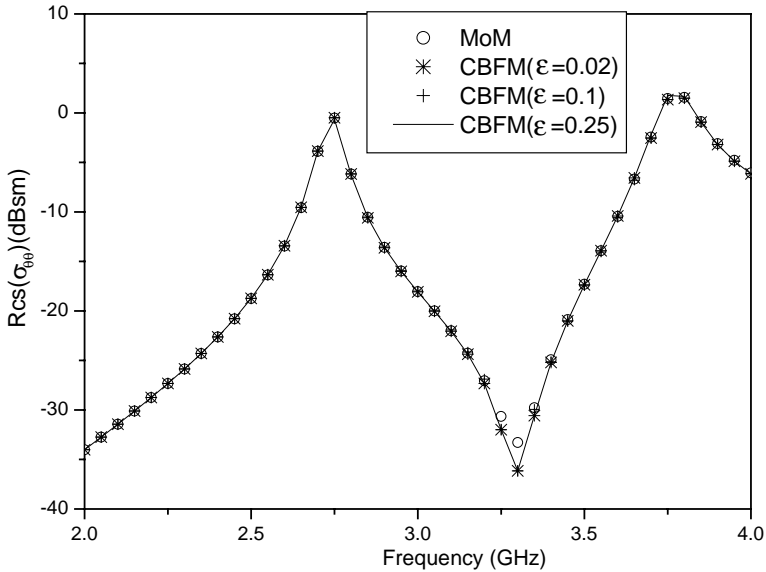


Figure 7. RCS versus frequency for the 3×3 array.

are divided into 9, 49 and 121 blocks respectively and lead to the same number of CBFs and the same size of reduced matrices. These small-size matrix equations can be computed using the direct solver. The RCS as a function of frequency is presented in Fig. 8, by using the present approach, along with the MoM solution and the results in [19]. An excellent agreement is showed over the entire frequency band.

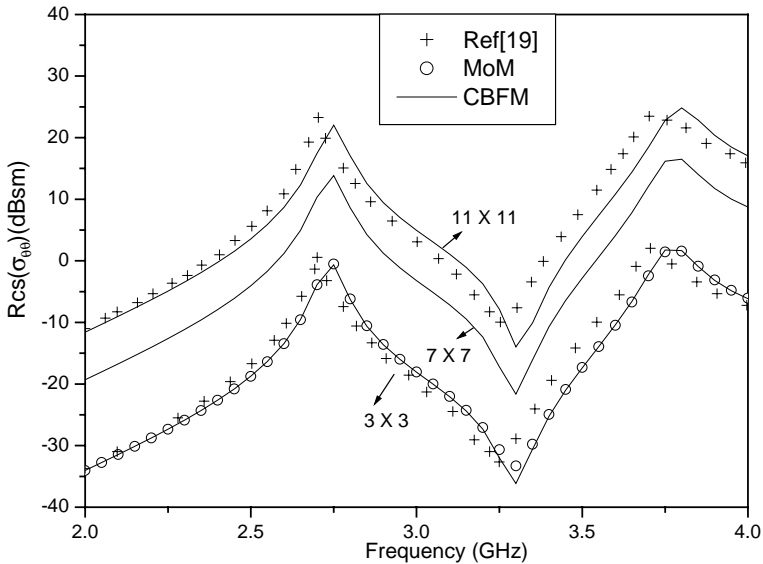
Having established the accuracy of the CBFM, we next examine the computational time involved in this technique. There are three main stages in the CBFM, namely, the fill of the block matrices, the generation of the CBFs, and the matrix reduction. The CPU times for these stages are presented in Table 1 for these three arrays. Note that the time for the LU decomposition of the block matrices is also included in the time for generating the CBFs. In addition, the total CPU time for CBFM solution is also given in this table for comparison with MoM. Obviously, this algorithm is more efficient.

The large RCS peaks at approximately 2.7 and 3.7 GHz correspond to the $(1, 0)$ and $(0, 1)$ cavity mode resonances, respectively. Hence the monostatic RCS ($\sigma_{\theta\theta}$) as functions of θ are also considered at these two frequency points. As shown in Fig. 9, since 2.7 GHz corresponds to the $(1, 0)$ cavity mode resonance, the broadside response is greatest at

Table 1. Computation of CPU time(s) for CBFM and MoM.

Examples	N	CBFM				MoM
		Block matrices	CBFs	Matrix reduction	Total time	
3×3 array	1737	23.23	0.11	0.6	24.05	357.73
7×7 array	9457	126.47	0.27	21.37	148.51	~
11×11 array	17787	186.36	0.33	85.47	272.76	~

In this table, symbol “~” means that the MoM solution of this array can not be obtained on our computer.

**Figure 8.** RCS versus frequency for various size arrays.

$\phi = 90^\circ$ and least at $\phi = 0^\circ$. Likewise, 3.7 GHz corresponds to the (0, 1) cavity mode resonance, the broadside response is greatest at $\phi = 90^\circ$ and least at $\phi = 0^\circ$ as shown in Fig. 10. The results obtained by King and Bow [19] and Ling and Jin [20] are also given in the figures for comparison. It is observed that our results agree very well with those given in [19] and [20].

It should be also shown that the CBFM is very suitable for many excitations vectors because the LU factors for the blocks matrices need not be computed repeatedly. Hence the computational time for the

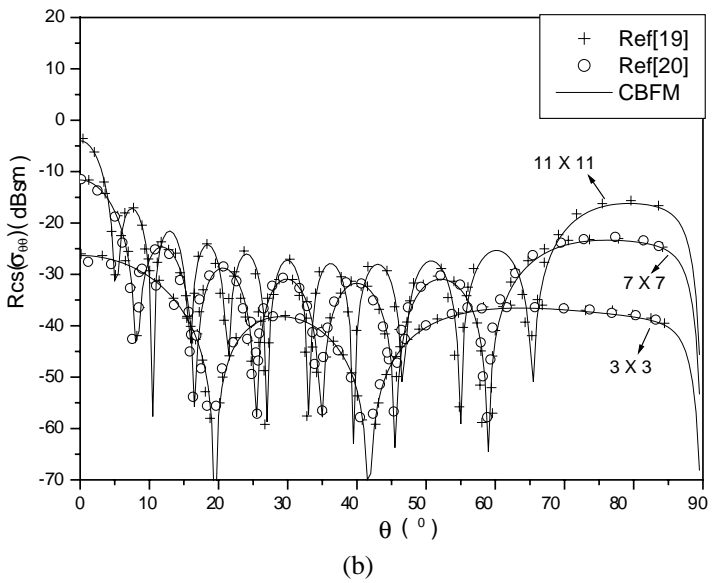
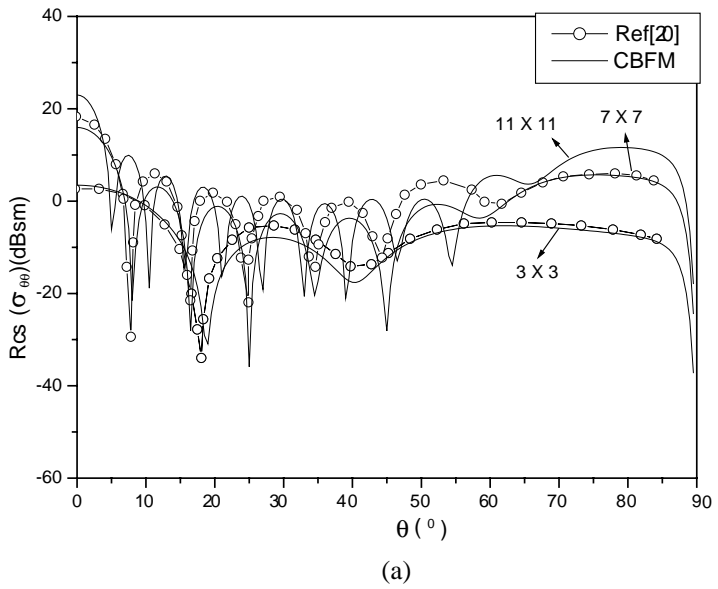


Figure 9. RCS versus θ for various size arrays at 2.7 GHz (a) $\phi = 0^\circ$ (b) $\phi = 90^\circ$.

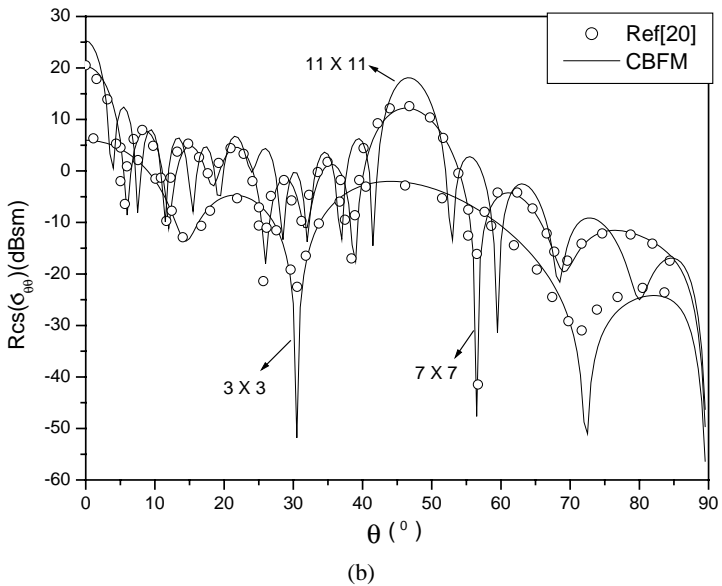
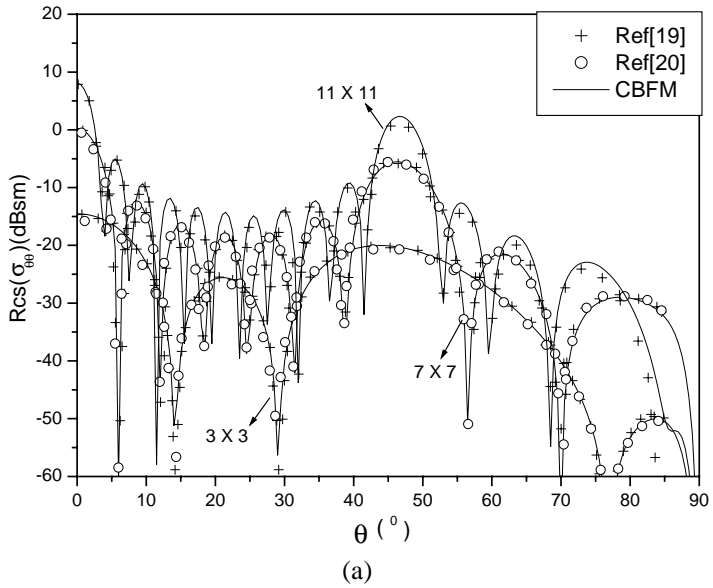


Figure 10. RCS versus θ for various size arrays at 3.7 GHz (a) $\phi = 0^\circ$ (b) $\phi = 90^\circ$.

other incident angles is less than that for the first incident angle. However, the solution times of iterative solvers for the second incident angle remain the same. And it is expected that the CBFM would show even more computational advantages over the iterative solvers for electrically large problems.

4. CONCLUSION

In this paper, we have proposed a novel scheme for the efficient MoM analysis of large-scale period planar arrays and antennas using the characteristic basis function method (CBFM). The accuracy of the proposed method has been verified by investigating several representative examples and excellent agreements for the S parameters and RCS have been achieved between the direct and CBF methods in all cases. The computation time as well as the memory requirements have been also compared to those of conventional direct computation. It is demonstrated that the use of CBFs can result in significant savings in computation time and memory requirements in our applications because identical block geometries and spacings between the array elements can be utilized. We have demonstrated that the CBFM is a very efficient approach and are expected to have applications in a wide variety of EM problems.

REFERENCES

1. Bleszynski, E., M. Bleszynski, and T. Jaroszewicz, "AIM: adaptive integral method for solving large-scale electromagnetic scattering and radiation problems," *Radio Sci.*, Vol. 31, 1225–1251, Sept./Oct. 1996.
2. Rokhlin, V., "Rapid solution of integral equations of scattering in two dimensions," *J. Comput. Phys.*, Vol. 86, 414–439, Feb. 1990.
3. Coifman, R., V. Rokhlin, and S. Wandzura, "The fast multipole method for the wave equation: A pedestrian prescription," *IEEE Antennas Propagat. Mag.*, Vol. 35, No. 3, 7–12, June 1993.
4. Song, J. M., C. C. Lu, and W. C. Chew, "Multilevel fast multipole algorithm for electromagnetic scattering by large complex objects," *IEEE Trans. Antennas Propagat.*, Vol. 45, No. 10, 1488–1493, Oct. 1997.
5. Canning, F. X., "The impedance matrix localization (IML) method for moment-method calculations," *IEEE Antennas Propagat. Mag.*, Vol. 32, 18–30, Oct. 1990.

6. Sarkar, T. K., E. Arvas, and S. M. Rao, "Application of FFT and the conjugate gradient method for the solution of electromagnetic radiation from electrically large and small conducting bodies," *IEEE Trans. Antennas Propagat.*, Vol. 34, No. 5, 635–640, May 1986.
7. Ling, F., J.-M. Song, and J.-M. Jin, "Multilevel fast multipole algorithm for analysis of large-scale microstrip structures," *IEEE Microwave Guided Wave Lett.*, Vol. 9, No. 12, 508–510, Dec. 1999.
8. Chow, Y. L., J. J. Yang, D. G. Fang, and G. E. Howard, "A closed-form spatial Green's function for the thick microstrip substrate." *IEEE Trans. Microwave Theory Tech.*, Vol. 39, No. 3, 588–592, Mar. 1991.
9. Howard, G. E. and Y. L. Chow, "Diakoptic theory for the microstrip structures," *IEEE AP-S Int. Symp. Dig.*, 1079–1082, Dallas, TX, May 1990.
10. Schwering, F., N. N. Puri, and C. M. Butler, "Modified Diakoptic theory of antennas," *IEEE Trans. Antennas Propagat.*, Vol. 34, 1273–1281, 1986.
11. Ooms, S. and D. D. Zutter, "A new iterative diakoptics-based multilevel moments method for planar circuits," *IEEE Trans. Microwave Theory Technol.*, Vol. 46, 280–291, 1998.
12. Suter, E. and J. R. Mosig, "A subdomain multilevel approach for the efficient MoM analysis of large planar antennas," *Microwave Opt. Technol Lett.*, Vol. 26, 270–277, 2000.
13. Kwon, S. J., K. Du, and R. Mittra, "Characteristic basis function method: A numerically efficient technique for analyzing microwave and RF circuits," *Microwave Optical Technol. Lett.*, Vol. 38, No. 6, 444–448, Sept. 2003.
14. Yeo, J., V. V. S. Prakash, and Ra. Mittra, "Efficient analysis of a class of microstrip antennas using the Characteristic basis function method (CBFM)," *Microwave Optical Technol Lett.*, Vol. 39, No. 6, 456–464, Dec. 2003.
15. Prakash, V. V. S. and R. Mittra. "Characteristic basis function method: A new technique for efficient solution of method of moments matrix equations," *Microwave Optical Technol Lett.*, Vol. 36, No. 2, 95–100, Jan. 2003.
16. Yeung, E. K. L. and J. R. Mosig, "Multilayer microstrip structure analysis with matched load simulation," *IEEE Trans. Antennas Propagat.*, Vol. 43, 143–149, Jan. 1995.
17. Mosig, J. R., "Arbitrarily shaped microstrip structures and their analysis with a mixed potential integral equation," *IEEE Trans.*

- Microwave Theory Tech.*, Vol. 36, 314–323, Feb. 1988.
18. Rao, S. M., D. R. Wilton, and A. W. Clisson, “Electromagnetic scattering by surfaces of arbitrary shape,” *IEEE Trans. Antennas and Propagat.*, Vol. 30, No. 3, 409–418, 1982.
 19. King, A. S. and W. J. Bow, “Scattering from a finite array of microstrip patches,” *IEEE Trans. Antennas Propagat.*, Vol. 40, No. 7, 770–774, July 1992.
 20. Ling, E. and J. M. Jin, “Scattering and radiation analysis of microstrip antennas using discrete complex image method and reciprocity theorem,” *Microwave Opt. Technol. Lett.*, Vol. 16, No. 4, 212–216, Nov. 1997.

Wan Jixiang was born in Henan, China, on May 25, 1978. He received the B.S. and M.S. degrees in electrical engineering from XiDian University, Xi’an, China, in 2000 and 2003, respectively. And he currently is pursuing Ph.D. degree at XiDian University. His research interests include numerical methods for electromagnetic, microstrip antennas, and microwave and millimeter-wave integrated circuits.

Lei Juan was born in Shanxi, China, 1979. She received the B.S. and M.S. degrees in electrical engineering from XiDian University, Xi’an, China, in 2000 and 2003, respectively. Since 2003, she has always worked at the national key laboratory of antennas and microwave technology at XiDian University. And her research interests include the analysis and design of phased arrays, waveguide slot antennas, microstrip antennas, and microwave integrated circuit analysis.

Liang Changhong was born in Shanghai, China, on December 9, 1943. He graduated in 1965 from the former Xidian University, Xi’an, China, and continued his graduate studies until 1967. From 1980 to 1982, he worked at Syracuse University Syracuse, New York, USA as a visiting scholar. He has been a professor and Ph.D. student advisor of Xidian University since 1986. He was awarded the titles “National Middle-Aged and Young Expert with Distinguished Contribution”, “National Excellent Teacher”, and “One of the 100 National Prominent Professors”, etc. Prof. Liang has wide research interests, which include computational microwave and computational electromagnetics, microwave network theory, microwave measurement method and data processing, lossy variational electromagnetics, electromagnetic inverse scattering, electromagnetic compatibility. Prof. Liang is a Fellow of CIE and a Senior Member of IEEE.